Supporting Material

Rosana Collepardo-Guevara[a], Tamar Schlick[a,b,*]

[a] *Department of Chemistry, New York University, 100 Washington Square East, New York, NY, 10003*
[b] *Courant Institute of Mathematical Sciences, New York University, 251 Mercer Street, New York, New York 10012*

---

*Corresponding author
Email address: schlick@nyu.edu (Tamar Schlick)

1. Further details on our computational methodology

Our integrated mesoscale model has been extensively validated against experimental measurements of sedimentation and diffusion coefficients, linear mass values, and other static and dynamic properties (1–4). For example, it reproduces salt-dependent sedimentation coefficients and packing ratios of chicken erythrocyte chromatin over a broad range of ionic environments with/without linker histones (3); salt-dependent extension of histone tails (2); the topology of chromatin fibers (2, 5, 6); and chromatin's internucleosome interaction patterns (4, 6).

Below, we provide further details in the different coarse-grained modeling strategies used for each component, the specific oligonucleosome energy expression, the Monte Carlo (MC) simulation protocol developed to sample equilibrium ensembles of chromatin configurations, and the analysis tools employed.

1.1. Chromatin Mesoscale Model

1.1.1. Nucleosome with flexible tails model

The nucleosome core, including the histone octamer without protruding tails and the 147 bp of DNA wound around it, is modeled as an irregularly-shaped electrostatic charged object. We use the discrete charge optimization (DiSCO) algorithm (7, 8) to define the values and positions of 300 Debye-Hückel charges evenly distributed over an irregular surface based on the nucleosome crystal structure (protein data bank entry 1KX5) (6). The DiSCO algorithm uses an optimization procedure that minimizes the error between the Debye-Hückel approximation and the electric field of the full atom representation of the nucleosome core at distances > 5Å. The optimization is achieved through the truncated-Newton TNPACK algorithm (9–11), as described in (7, 8). The electric field is computed using the nonlinear Poisson-Boltzmann equation solver QNIFFT 1.2 (12–14). The atomic radii input for QNIFFT is taken from the default extended atomic radii loosely based on M. Conolly's Molecular Surface program (15), and the charges taken from the AMBER 1995 force field (16). As discussed elsewhere (17), agreement between the Debye-Hückel electric field and that obtained by solving the complete Poisson-Boltzmann equation is excellent for this number of pseudo-charges.

We attach ten flexible histone tails to their idealized positions in the nucleosome crystal structure. Each tail is treated with a protein-bead chain model

as developed in (2). In this model, five adjacent amino acids are represented using a single bead located at the C_β atom of the central amino acid. The number of beads for each of the two $H2A_1$ (N-termini), $H2A_2$ (C-termini), H2B, H3 and H4 histone tails is 4, 3, 5, 8, and 5, respectively, yielding a total of 50 beads per nucleosome (Figure 1) (2, 18). The parameterized histone tail bead stretching and bending harmonic potentials reproduce configurational properties of the atomistic histone tails via Brownian dynamics simulations (2). Each histone tail bead is assigned a charge equal to the sum of the charges on the five amino acids it represents. The electrostatic interactions in the presence of salt are modeled by multiplying the charges by a scaling factor close to unity that reproduces the electric field of the atomistic model (18). For the salt concentration of 0.15 M used here, the scaling factor is 1.12.

1.1.2. Linker DNA model

The entering and exiting DNA linkers attached to each nucleosome (other than the first) are modeled as elastic worm-like chains of N_{DNA} spherical beads each (19, 20). The repeating sequence of one nucleosome particle followed by N_{DNA} DNA beads forms the main N_c-core oligonucleosome chain; the first bead in the chain ($i = 1$) represents the first core, and the last bead ($i = N$ with $N = N_c*(N_{\mathrm{DNA}}+1)$) the last linker DNA bead (as illustrated in Supporting Figure 1a). The nucleosome points of attachment of the exiting and entering DNA linkers enclose an angle ϕ_0=108° about the center of the nucleosome and are separated by a distance 3.6 nm normal to the plane of the nucleosome core, consistently with the nucleosome crystal structure (21). Each DNA linker bead has an internal force field comprising of stretching, bending, and twisting potential energy terms. Each bead also carries a salt-dependent negative charge assigned through the Stigter's procedure to mimic the electrostatic potential of linear DNA (22). The DNA inter-bead segments have an equilibrium length (l_0) of 3 nm, which determines the values of the NRL that we can model (6). The NRL is calculated from the number of inter-bead segments ($N_S = N_{\mathrm{DNA}} + 1$) as NRL = 147 bp + $N_S l_0/a$, where $a = 0.34$ nm/bp is the rise per base pair. Here, we study systems of 3 and 7 inter-bead segments (2 and 6 DNA beads), which correspond to NRLs of 173 and 209 bp, respectively.

In chromatin, the double stranded linker DNA is twisted about the DNA axis with a helical repeat of 10.3 bp/turn (l_r) (23, 24). Thus, the DNA linker length determines the number of turns between nucleosome cores. The

number of turns can be calculated as (NRL − 147 bp)/l_r (6). When a linker DNA makes m integral turns ($m = 1, 2, \dots$), its average twist is zero, and when it makes a non-integral $m + r$ (with $r \in (0, 1)$) number of turns, its average twist is equal to $360°(r - 1)$. Our approach assigns the appropriate average equilibrium twist value per DNA linker segment (ϕ_{N_S}) through a twisting energy deformation (6). For example, our DNA linkers of 7 and 3 segments (NRLs ∼209 and 173 bp, respectively) studied here, complete 6 and 2.43 turns, respectively. This corresponds to ϕ_{N_S}=0 for NRL = 209 bp, and ϕ_{N_S}= 51.7°, or an average DNA twist of $-0.57 \times 360° = 155°$ for the whole 173-bp linker segment. See more details in Ref. (6).

1.2. Initial configurations

For our initial configurations, we have used representative equilibrium conformations simulated previously in the presence of LH (1 per core) at 0.15 M NaCl and 293 K, and zero pulling force (6). These equilibrium conformations were obtained by running MC trajectories for 35 million steps starting from idealized zigzag and interdigitated solenoid conformations. For the NRLs studied here, both starting conformations (zigzag and solenoid) give equilibrium structures with interaction patterns and geometrical descriptors characteristic of zigzag fibers (6). Therefore, although our initial configurations in this work have dominant zigzag interactions, these are configurations determined by modeling as the most favorable and not idealized two-start conformations.

1.3. Analysis tools

1.3.1. Force-Distance curve

The main output of a single-molecule stretching assay is the so-called Force-Distance or Force-Extension (F-D) curve, that gives information of the force necessary to stretch a system by a specific distance. We compute F-D curves by applying a constant pulling force and evaluating the ensemble average of the resulting end-to-end distance in the direction of the applied force. This distance here is the end-to-end distance in the z-direction between the geometric centers of the first and last nucleosome cores.

1.3.2. Patterns of internucleosome interactions

To describe the internal organization of the nucleosomes in an oligonucleosome we construct a two-dimensional *interaction-intensity matrix*, $I'(i, j)$ that measures the intensity of histone-tail mediated interactions between

nucleosomes i and j. Each matrix element is obtained by calculating the fraction of MC iterations that the two cores are in contact with one another:

$$I'(i,j) = \text{mean}\left[\delta_{i,j}(M)\right], \tag{1}$$

where M is the MC configurational frame. The mean is calculated over the converged MC frames used for statistical analysis, with

$$\delta_{i,j}(M) = \begin{cases} 1 & \text{if cores } i \text{ and } j \text{ are 'in contact' at MC frame } M, \\ 0 & \text{otherwise.} \end{cases} \tag{2}$$

Nucleosomes i and j are 'in contact' if the shortest distance between the tail-beads directly attached to i and the tail-beads or core-charges of core j is smaller than the excluded volume distance (σ_t=1.8 nm) (2). Finally, these matrices are projected into unnormalized one-dimensional maps

$$I(k) = \frac{1}{N_C} \sum_{i=1}^{N_C} I'(i, i \pm k) \tag{3}$$

that describe the relative intensity of the interactions between cores separated by k DNA linkers and reveal the pattern of internucleosome interactions (dominant, moderate, weak) in a chromatin fiber. The ideal two-start zigzag configuration has dominant $i \pm 2$ and moderate $i \pm 5$ interactions, while the ideal 6-nucleosomes per turn solenoid model has dominant $i \pm 1$ interactions (6).

1.3.3. Internucleosome interaction energy

We monitor the behavior of the stabilizing internucleosome interaction energy during the pulling process. We define this term as the ensemble average of the total electrostatic interaction energy between nucleosome pairs divided over the total number of cores.

2. Chromatin energy

The total potential energy of our oligonucleosomes is a sum of twisting, stretching and bending energy of the linker DNA, stretching and intramolecular bending of the linker histones and histone tails, total electrostatic energy, and excluded volume contributions:

$$E = E_T + E_S + E_B + E_{tS} + E_{tB} + E_{LH} + E_C + E_V. \quad (4)$$

The mechanical potential of the DNA is implemented by assigning local coordinate systems to all DNA linker beads and the nucleosome cores. The center position of each chain bead i (nucleosome core or DNA linker bead) is described by the vector $\mathbf{r}_i = (x_i, y_i, z_i)$, and its coordinate system is specified by three orthonormal unit vectors $\{\mathbf{a}_i,\mathbf{b}_i,\mathbf{c}_i\}$, where $\mathbf{c}_i = \mathbf{a}_i \times \mathbf{b}_i$ (see Figure 2). Each nucleosome core i has three additional coordinate systems that describe the DNA bending and twisting at their points of attachment to the nucleosome: $\{\mathbf{a}_i^{\mathrm{DNA}},\mathbf{b}_i^{\mathrm{DNA}},\mathbf{c}_i^{\mathrm{DNA}}\}$ represents the direction from the attachment point of the exiting linker DNA to the center of the $i+1$ DNA bead; $\{\mathbf{a}_i^{+},\mathbf{b}_i^{+},\mathbf{c}_i^{+}\}$ represents the local tangent on the nucleosome core at the point of attachment of the exiting linker DNA; and $\{\mathbf{a}_i^{-},\mathbf{b}_i^{-},\mathbf{c}_i^{-}\}$ represents the tangent vector corresponding to the entering linker DNA. The Euler angles α_i, β_i, and γ_i transform the coordinate system of one linker DNA to that of the next (or to that of the entering point of attachment to the core) along the oligonucleosome chain (i.e., $\{\mathbf{a}_i,\mathbf{b}_i,\mathbf{c}_i\} \rightarrow \{\mathbf{a}_{i+1},\mathbf{b}_{i+1},\mathbf{c}_{i+1}\}$); angles α_i^{+}, β_i^{+}, and γ_i^{+} transform the coordinate system of the nucleosome core to that of the exiting linker DNA (i.e., $\{\mathbf{a}_i,\mathbf{b}_i,\mathbf{c}_i\} \rightarrow \{\mathbf{a}_i^{\mathrm{DNA}},\mathbf{b}_i^{\mathrm{DNA}},\mathbf{c}_i^{\mathrm{DNA}}\}$). Further details on the Euler angles and a geometric description of the oligonucleosome chain are provided in (3, 6, 17).

The first term in Eq. (4) is the twisting energy of the DNA. This term incorporates the appropriate equilibrium twist per DNA linker segment to accommodate non-integral numbers of DNA turns:

$$E_T = \frac{s}{2l_0} \sum_{i=1}^{N-1} \left(\alpha_i + \gamma_i - \phi_{N_S}\right)^2, \quad (5)$$

where s is the twisting rigidity of DNA, n is the number of beads in the oligonucleosome chain, ϕ_{N_s} is the twist deviation penalty term per segment, and the sum $\alpha_i + \gamma_i$ gives the linker DNA twist at each bead location. The next two terms denote the stretching,

$$E_S = \frac{h}{2} \sum_{i=1}^{N-1} \left(l_i - l_0\right)^2, \quad (6)$$

and bending energy of the linker DNA,

$$E_B = \frac{g}{2}\left[\sum_{i=1}^{N}(\beta_i)^2 + \sum_{i=i\in I_C}^{N}\left(\beta_i^+\right)^2\right]. \tag{7}$$

Here h and g are the stretching and bending rigidities of DNA, $l_i = |\mathbf{r}_{i+1} - \mathbf{r}_i|$ the separation between consecutive DNA beads, and I_C denotes a nucleosome particle within the oligonucleosome chain (see Supporting Table 1). The Euler angles β_i and β_i^+ are bending angles, and l_0 is the equilibrium separation distance between beads of relaxed DNA, as given above.

The fourth term, E_{tS}, represents the total stretching energy of the histone tails:

$$E_{tS} = \sum_{i\in I_C}^{n}\sum_{j=1}^{N_T}\sum_{k=1}^{N_{bj}-1}\frac{k_{b_{jk}}}{2}\left(l_{ijk} - l_{jk0}\right)^2 + \frac{h_{tc}}{2}\sum_{i\in I_C}^{N}\sum_{j=1}^{N_T}\left|\mathbf{t}_{ij} - \mathbf{t}_{ij0}\right|^2. \tag{8}$$

Here $N_T = 10N_C$ is the total number of histone tails, N_{bj} is the number of beads in the j-th tail, and $k_{b_{jk}}$ is the stretching constant of the bond between the k-th and $k+1$-th beads of the j-th histone tail. l_{ijk} and l_{jk0} represent the distance between tail beads k and $k+1$, and their equilibrium separation distance, respectively. In the second term, h_{tc} is the stretching bond constant of the spring attaching the histone tail to the nucleosome core, $\mathbf{t}_{ij}$ is the position vector of the first tail bead in the coordinate system of its parent nucleosome, and $\mathbf{t}_{ij0}$ is the position vector of the attachment site to the nucleosome core.

The fifth term, E_{tB}, represents the intramolecular bending contribution to the histone tail energies:

$$E_{tB} = \sum_{i\in I_C}^{N}\sum_{j=1}^{N_T}\sum_{k=1}^{N_{bj}-2}\frac{k_{\theta_{jk}}}{2}\left(\theta_{ijk} - \theta_{jk0}\right)^2, \tag{9}$$

where θ_{ijk} and θ_{jk0} represent the angle between three consecutive tail beads (k, $k+1$, and $k+2$) and their equilibrium angle, respectively, $k_{\theta_{jk}}$ is the corresponding bending force constant.

The sixth term, E_{LH}, represents the intramolecular stretching and bending energy of the linker histone beads:

$$E_{LH} = \sum_{i\in I_C}^{N}\sum_{k=1}^{2}\frac{k_S^{LH}}{2}\left(l_{ik}^{LH} - l_0^{LH}\right)^2 + \sum_{i\in I_C}^{N}\frac{k_\theta^{LH}}{2}\left(\theta_i^{LH} - \theta_0^{LH}\right)^2. \tag{10}$$

Here, k_S^{LH} is the stretching constant between consecutive LH beads of a given core, and l_{ik}^{LH} and $l_0^{LH} = 2.6$ nm represent the distance between histone beads k and $k+1$, and their equilibrium separation distance, respectively. In the second term, θ_i^{LH} represents the angle between the three consecutive histone beads (k, k+1, and k+2) of core i, $\theta_0^{LH} = 2\pi$ is the equilibrium angle between LH beads, and $k_{\theta^{LH}}$ is the corresponding bending force constant. To allow only a moderate stretching and bending flexibility among LH beads, the force constants have been empirically set to be one order of magnitud higher than the equivalent constants for histone tail motions (i.e. $k_S^{LH} = 10 \max(k_{b_{jk}})$ and $k_{\theta^{LH}} = 10 \max(k_{\theta_{jk}})$).

The total electrostatic interaction energy of the oligonucleosome is given by E_C. These include ten types of interactions: nucleosome / nucleosome, nucleosome / linker-DNA, nucleosome / tail, nucleosome / linker-histone, linker-DNA / tail, linker-DNA / linker-DNA, linker-DNA / linker-histone, tail / tail, tail / linker-histone, and linker-histone / linker-histone. All these interactions are modeled using the Debye-Hückel potential that accounts for salt screening:

$$E_C = \sum_i \sum_{j \neq i} \frac{q_i q_j}{4\pi\epsilon\epsilon_0 r_{ij}} \exp\left(-\kappa r_{ij}\right), \tag{11}$$

where q_i and q_j are the 'effective' charges separated by a distance r_{ij} in a medium with a dielectric constant of ϵ and a salt-concentration dependent inverse Debye length of κ, ϵ_0 is the electric permittivity of vacuum. Within an individual linker-DNA chain or histone-tail chain, the beads belonging to the same chain do not interact electrostatically with each other as their interactions are already accounted through the intramolecular force field (harmonic spring). Finally, linker DNA beads, linker histone beads, and histone tail beads directly attached to the nucleosome do not interact electrostatically with their parental nucleosomal pseudo-charges. This is required to ensure that the attachment tail and linker DNA beads remain as close as possible to their equilibrium locations.

The last term, E_V, represents the total excluded volume interaction energy of the oligonucleosome. The excluded volume interactions are modeled using the Lennard-Jones potential and the total energy is given by:

$$E_V = \sum_i \sum_{j \neq i} k_{ij} \left[\left(\frac{\sigma_{ij}}{r_{ij}} \right)^{12} - \left(\frac{\sigma_{ij}}{r_{ij}} \right)^{6} \right], \tag{12}$$

where σ_{ij} is the effective diameter of the two interacting beads and k_{ij} is an

energy parameter that controls the steepness of the excluded volume potential. These parameters are taken from relevant models of the components as tabulated in Supporting Tables 1 to 3 below (see further details on parameters in (3)).

2.1. Monte Carlo sampling

To sample the ensemble of oligonucleosome conformations at constant temperature we use MC simulations with five different MC moves (global pivot, local translation, local rotation, tail regrowth and LH reorganization) and one optional MC move (LH on and off). These moves are detailed below.

- *Pivot, translation, and rotation chain moves.* The global pivot move is implemented by randomly choosing one linker DNA bead or nucleosome core and a random axis passing through the chosen component. The shorter part of the oligonucleosome about this axis is rotated by an angle chosen from a uniform distribution within [0, 20°]. The local translation and rotation moves also select randomly a oligonucleosome chain component (linker DNA bead or core) and an axis passing through it. In translation, the component is moved along the axis by a distance sampled from a uniform distribution within [0, 0.6 nm]. In the rotation move, the component is rotated about the axis by an angle sampled from an uniform distribution in the range [0, 36°]. All three MC moves are accepted or rejected based on the Metropolis criterion.

- *Tail regrowth move.* The tail regrowth move is implemented to sample histone-tail conformations based on the configurational bias MC method (25, 26). It randomly selects a histone tail chain and regrows it bead-by-bead using the Rosenbluth scheme (27). To prevent histone tail beads from penetrating the nucleosome core, the volume enclosed within the nucleosome surface is discretized, and any trial configurations that place the beads within this volume are rejected automatically.

- *LH reorganization move.* The LH reorganization move is implemented by randomly selecting one LH bead and and axis passing through it, and then translating the bead along that axis by a distance sampled from a uniform distribution within [0, 0.3 nm]. As done in the tail regrowth move, any trial configurations that place the LH beads within the nucleosome discretized volume are rejected automatically. The rest of the trial configurations are selected based on the Metropolis criterion.

- *LH on and off move.* This LH stop-and-go move attaches or detaches a full LH chain from its parent core. One LH is selected at random. If the LH is bound to a core, a trial configuration is formed by either leaving the LH bound or, with a probability $p_d \in (0, 1)$, detaching it and diffusing it to infinity so that the contribution to the total energy of the selected LH is zero. If the LH is unbound, the trial configuration is formed by reattaching the LH to its core with a probability $p_a \in (0, 1)$. The trial configuration is then accepted or rejected based on the Metropolis criterion. The values of p_d and p_a give the dissociation-and-diffusion and association probabilities, respectively, and affects the average number of LH-core bonds present in a fiber at a given MC time. Here, we model two cases: (a) $p_a >> p_d$ (i.e., p_a=1 and p_d=0.25), and (b) $p_a = p_d$ (i.e., p_a=1 and p_d=1). When $p_a = p_d = 1$, the LH follow a slow rebinding scenario and produce oligonucleosome conformations in which LH follow a slow binding mode and ∼50% of LH are bound to cores. When p_a=1 and p_d=0.25, we reproduce LH's fast binding mode behavior, in which the unbound LH molecules have a much higher probability of rebinding to cores than diffusing to infinity; this produces an equilibrium oligonucleosome conformations in which the majority (∼80%) of LH proteins are bound to cores, and the LH-core bonds are exchanged among the ensemble of conformations.

The pivot, translation, rotation, tail regrowth, and LH reorganization moves are attempted with probabilities of 0.2, 0.1, 0.1, 0.4, and 0.2, respectively (3). In simulations that consider LH dynamic binding, the probabilities for the pivot, translation, rotation, tail regrowth, LH reorganization, and LH on and off moves are 0.2, 0.1, 0.1, 0.4, 0.1, and 0.1, respectively.

Parameter	Description	Value
T	Temperature	293.15° K
C_S	Monovalent salt concentration (NaCl)	0.15 M
l_0	Equilibrium DNA segment length	3.0 nm
L_p	Persistence length of linker DNA in monovalent salt	50 nm
h	Stretching rigidity of linker DNA	$100k_B\mathrm{T}/l_o^2$
g	Bending rigidity of linker DNA	$L_pk_B\mathrm{T}/l_o$
s	Torsional rigidity constant of linker DNA	3.0×10^{-12} erg.nm
θ_0	Angular separation between linker segments at core	108°
$2w_0$	Width of wound DNA supercoil	3.6 nm
r_0	Radius of wound DNA supercoil	4.8 nm
σ_{tt}	Excluded vol. distance for tail/tail interactions	1.8 nm
σ_{tc}	Excluded vol. distance for tail/core interactions	1.8 nm
σ_{cc}	Excluded vol. distance for core/core interactions	1.2 nm
σ_{tl}	Excluded volume distance for tail/linker DNA interactions	2.7 nm
σ_{cl}	Excluded vol. distance for core/linker DNA interactions	2.4 nm
σ_{gLHc}	Excluded vol. distance for globular link. hist./core interactions	2.2 nm
σ_{gLH1}	Excluded vol. distance for globular link. hist./link.DNA interactions	3.4 nm
σ_{cLHc}	Excluded vol. distance for C-term. link. hist./core interactions	2.4 nm
σ_{cLH1}	Excluded vol. distance for C-term. link. hist./link.DNA interactions	3.6 nm
k_{ev}	Excluded vol. energy param for all components except for tail beads	0.001 k_BT
k_{evt}	Tail/tail excluded volume interaction energy parameter	0.1 k_BT
q_{gLH}	Charge on the globular linker histone bead	13.88e
q_{cLH}	Charge on the C-terminal linker histone bead	25.62e
σ_{LHLH}	Excluded volume distance for link.histone/link.histone interactions	2.0 nm

Supporting Table 1: Parameters employed in mesoscale modeling/simulation.

Tail	Bond i-j	k_b (kcal/mol/Å^2)	Average [Å]	SD [Å]
N-ter H3	1-2	0.09	15.6	2.3
	2-3	0.06	15.0	3.0
	3-4	0.07	15.6	2.9
	4-5	0.07	16.1	2.6
	5-6	0.07	16.1	2.6
	6-7	0.07	15.1	2.9
	7-8	0.11	14.9	2.4
N-ter H4	1-2	0.10	14.1	2.6
	2-3	0.10	15.2	2.4
	3-4	0.06	14.8	2.8
	4-5	0.20	14.7	1.8
N-ter H2A	1-2	0.08	14.1	2.6
	2-3	0.09	15.3	2.5
	3-4	0.03	14.5	3.4
C-ter H2A	1-2	0.07	15.7	2.6
	2-3	0.07	13.7	2.6
N-ter H2B	1-2	0.08	14.7	3.1
	2-3	0.10	14.1	2.3
	3-4	0.08	16.2	2.4
	4-5	0.08	15.1	2.7

Supporting Table 2: Protein bead stretching parameters.

Tail	Angle i-j-k	k_θ (kcal/mol/rad^2)	Average [°]	SD [°]
N-ter H3	1-2-3	1.1	108.6	28.8
	2-3-4	1.0	108.1	28.6
	3-4-5	1.7	111.3	25.4
	4-5-6	1.2	117.6	27.8
	5-6-7	1.2	110.4	29.3
	6-7-8	1.5	110.5	27.2
N-ter H4	1-2-3	1.0	103.2	25.4
	2-3-4	1.1	106.0	25.8
	3-4-5	0.5	103.6	35.5
N-ter H2A	1-2-3	1.1	108.5	29.0
	2-3-4	0.6	100.1	29.3
C-ter H2A	1-2-3	1.0	100.7	31.8
N-ter H2B	1-2-3	0.9	104.9	35.1
	2-3-4	0.6	103.9	28.4
	3-4-5	1.6	113.8	26.7

Supporting Table 3: Protein bond-angle parameters.

References

1. Arya, G., Q. Zhang, and T. Schlick, 2006. Flexible histone tails in a new mesoscopic oligonucleosome model. *Biophys J* 91:133–150.

2. Arya, G., and T. Schlick, 2006. Role of histone tails in chromatin folding revealed by a mesoscopic oligonucleosome model. *Proc Natl Acad Sci USA* 103:16236–16241.

3. Arya, G., and T. Schlick, 2009. A tale of tails: how histone tails mediate chromatin compaction in different salt and linker histone environments. *J Phys Chem A* 113:4045–4059.

4. Grigoryev, S. A., G. Arya, S. Correll, C. L. Woodcock, and T. Schlick, 2009. Evidence for heteromorphic chromatin fibers from analysis of nucleosome interactions. *Proc Natl Acad Sci USA* 106:13317–13322.

5. Schlick, T., and O. Perišić, 2009. Mesoscale simulations of two nucleosome-repeat length oligonucleosomes. *Phys Chem Chem Phys* 11:10729–10737.

6. Perišić, O., R. Collepardo-Guevara, and T. Schlick, 2010. Modeling studies of chromatin fiber structure as a function of DNA linker length. *J Mol Biol* 403:777–802.

7. Beard, D. A., and T. Schlick, 2001. Modeling salt-mediated electrostatics of macromolecules: the discrete surface charge optimization algorithm and its application to the nucleosome. *Biopolymers* 58:106–115.

8. Zhang, Q., D. A. Beard, and T. Schlick, 2003. Constructing irregular surfaces to enclose macromolecular complexes for mesoscale modeling using the Discrete Surface Charge Optimization (DiSCO) algorithm. *J Compt Chem* 24:2063–2074.

9. Schlick, T., and M. Overton, 1987. A powerful truncated Newton method for potential energy minimization. *J Comp Chem* 8:1025–1039.

10. Schlick, T., and A. Fogelson, 1992. TNPACK - A truncated Newton minimization package for large scale problems: I. Algorithm and usage. *ACM Trans Math Softw* 18:46–70.

11. Schlick, T., and A. Fogelson, 1992. TNPACK - A truncated Newton minimization package for large scale problems : II. Implementation examples. *ACM Trans Math Softw* 18:71–111.

12. Gilson, M. K., K. A. Sharp, and B. H. Honig, 1988. Calculating the electrostatic potential of molecules in solution: Method and error assessment. *J Comp Chem* 9:327–335.

13. Sharp, K. A., and B. Honig, 1990. Electrostatic interactions in macromolecules: theory and applications. *Annu Rev Biophys Biophys Chem* 19:301–332.

14. Sharp, K. A., and B. Honig, 1990. Calculating total electrostatic energies with the nonlinear Poisson-Boltzmann equation. *J Phys Chem* 94:7684–7692.

15. Connolly, M. L., 1983. Solvent-accessible surfaces of proteins and nucleic acids. *Science* 221:709–713.

16. Cornell, W. D., P. Cieplak, C. I. Bayly, I. R. Gould, K. M. Merz, D. M. Ferguson, D. C. Spellmeyer, T. Fox, J. W. Caldwell, and P. A. Kollman, 1995. A second generation force field for the simulation of proteins, nucleic acids, and organic molecules. *J Am Chem Soc* 117:5179–5197.

17. Beard, D. A., and T. Schlick, 2001. Computational modeling predicts the structure and dynamics of chromatin fiber. *Structure* 9:105–114.

18. Arya, G., and T. Schlick, 2007. Efficient global biopolymer sampling with end-transfer configurational bias Monte Carlo. *J Chem Phys* 126:044107.

19. Allison, S., R. Austin, and M. Hogan, 1989. Bending and twisting dynamics of short linear DNAs. Analysis of the triplet anisotropy decay of a 209 base pair fragment by Brownian simulation. *J Chem Phys* 90:3843–3854.

20. Heath, P. J., J. A. Gebe, S. A. Allison, and J. M. Schurr, 1996. Comparison of analytical theory with Brownian dynamics simulations for small linear and c ircular DNAs. *Macromolecules* 29:3583–3596.

21. Davey, C. A., D. F. Sargent, K. Luger, A. W. Maeder, and T. J. Richmond, 2002. Solvent mediated interactions in the structure of the nucleosome core particle at 1.9 Å resolution. *J Mol Biol* 319:1097–1113.

22. Stigter, D., 1977. Interactions of highly charged colloidal cylinders with applications to double-stranded. *Biopolymers* 16:1435–1448.

23. Drew, H. R., and A. A. Travers, 1985. DNA bending and its relation to nucleosome positioning. *J Mol Biol* 186:773–790.

24. Deng, J., B. Pan, and M. Sundaralingam, 2003. Structure of d(ITITACAC) complexed with distamycin at 1.6 Å resolution. *Acta Cryst D* 59:2342–2344.

25. Frenkel, D., G. C. A. Mooij, and B. Smit, 1992. Novel scheme to study structural and thermal-properties of continuously deformable molecules. *J Phy Cond Matt* 4:3053–3076.

26. de Pablo, J. J., M. Laso, and U. W. Suter, 1992. Simulation of polyethylene above and below the melting point. *J Chem Phys* 96:2395–2403.

27. Rosenbluth, M. N., and A. W. Rosenbluth, 1955. Monte Carlo calculation of the average extension of molecular chains. *J Chem Phys* 23:356–359.

28. Cui, Y., and C. Bustamante, 2000. Pulling a single chromatin fiber reveals the forces that maintain its higher-order structure. *Proc Natl Acad Sci USA* 97:127–132.

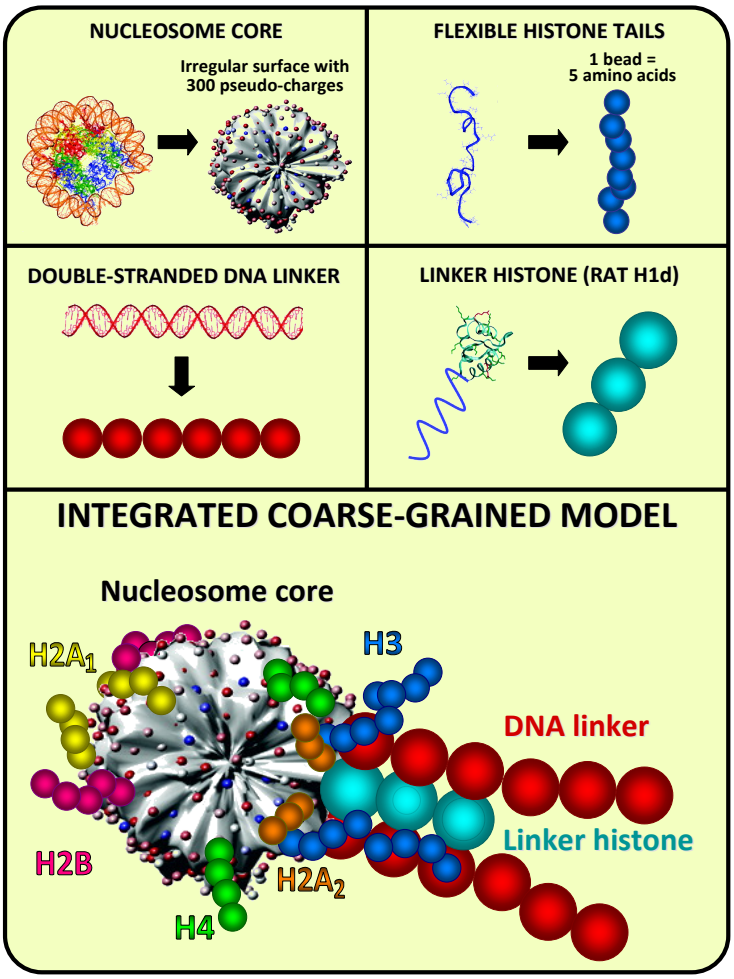

Supporting Figure 1: Mesoscale model of the basic chromatin building block. The nucleosome core surface with wrapped DNA without histone tails is modeled as an irregularly shaped rigid body with 300 optimized pseudo surface charges (small white, pink, magenta, and blue spheres). The linker DNA (large red spheres) is treated using the discrete worm like chain model. The histone tails are coarse-grained as bead models (medium spheres / $H2A_1$: yellow, $H2A_2$: orange, H2B: magenta, H3: blue, H4: green). The LH is modeled as 3 charged beads rigidly connected to the nucleosome (turquoise spheres).

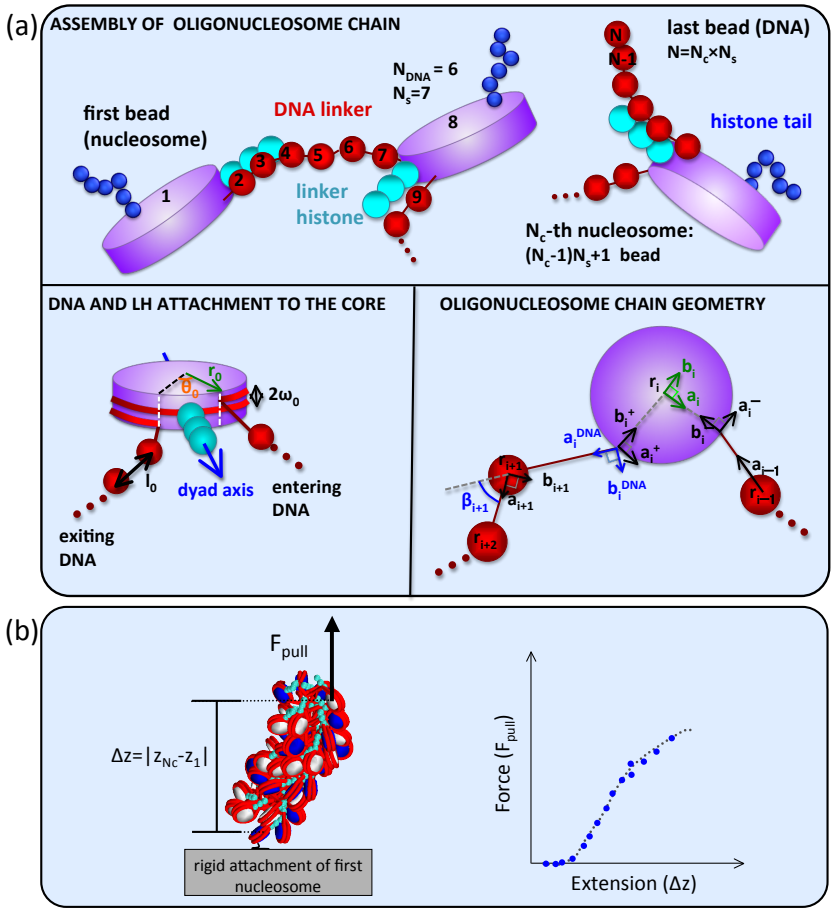

Supporting Figure 2: Top: Geometry of the mesoscale oligonucleosome model. (a) Shown is the assembly of oligonucleosome components into a chain, entering/exiting linker DNA, and individual coordinate systems for the linker DNA beads and nucleosome core, and Euler angle β depicting the linker DNA bending. For nucleosome core i, $\mathbf{a}_i$ and $\mathbf{b}_i$ lie in the nucleosome core plane, with $\mathbf{a}_i$ pointing along the tangent at the attachment site of the entering DNA, and $\mathbf{b}_i$ in the direction normal to this tangent. For linker DNA bead i, the vector $\mathbf{a}_i$ points from the geometric center of i to either the center of the following DNA bead or to the attachment point in the nucleosome (if $i+1$ is a core). The vector $\mathbf{a}_i^{\mathrm{DNA}}$ points from the attachment point of the exiting linker DNA to the center of the following DNA linker bead. The vectors $\mathbf{a}_i^+$ and $\mathbf{a}_i^-$ represent the local tangents on the nucleosome cores at the exiting and entering points of attachment, respectively. (b) Schematic representation of a pulling experiment.

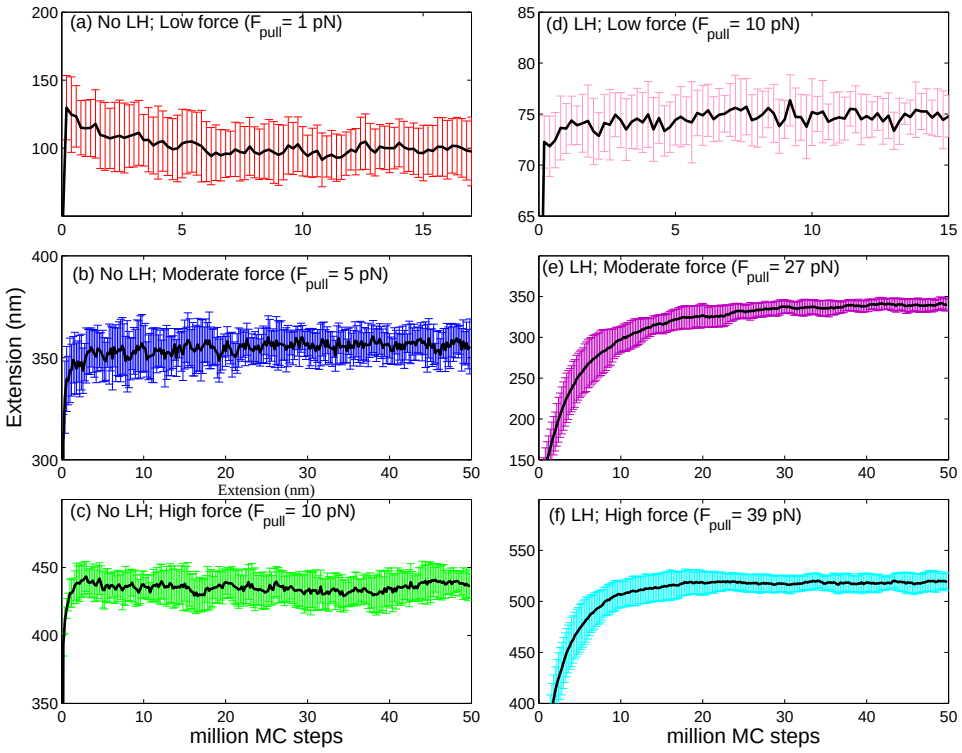

Supporting Figure 3: Behavior of the end-to-end distance for 24-unit 209-bp oligonucleosomes with/without LH subjected to different pulling forces: (a) without LH at low force (1 pN), (b) without LH at moderate force (5 pN), (c) without LH at high force (10 pN), (d) with 1 fixed LH/core at low force (10 pN), (b) with 1 fixed LH at moderate force (27 pN), and (c) with 1 LH/core at high force (39 pN). Convergence is evident well before 45 million MC steps for all cases shown.

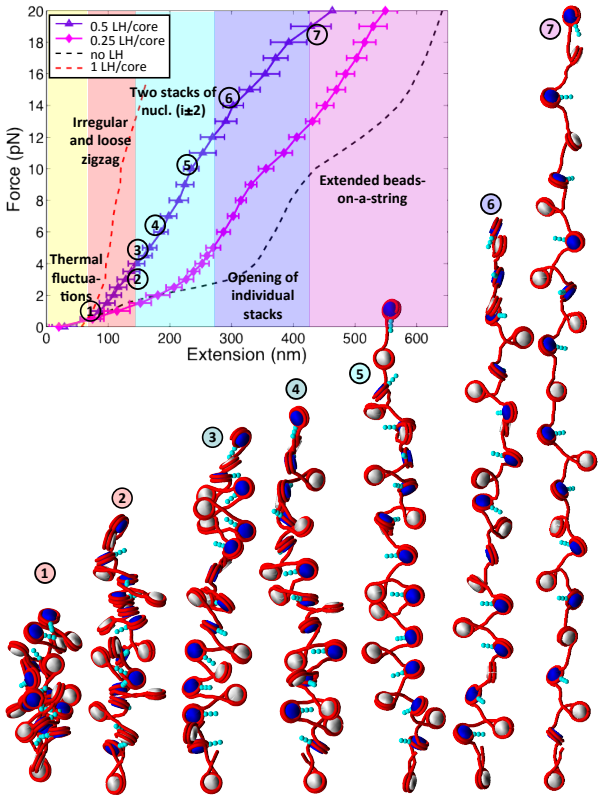

Supporting Figure 4: Force-extension curve of 209-bp 24-unit oligonucleosome chains at 0.15 M monovalent salt with 0.5 fixed LH/core and 0.25 fixed LH/core. The space filling models are based on MC stretching simulation snapshots of 0.5 fixed LH/core arrays. Alternating nucleosomes are colored white and navy, with wrapped DNA as red. LH is shown as three turquoise spheres. Lower LH stoichiometries of 0.5 and 0.25 fixed LH/core decrease significantly the stiffness of medium-NRL fibers, as revealed by their lower elastic moduli (σ ~5 pN and σ ~2 pN, respectively) compared to that of 1 LH/core fibers (σ ~10 pN); note that the stiffness of fibers with 0.25 LH/core is comparable to that of fibers without LH. Moreover, the detailed unfolding mechanism also changes when the LH/core ratio decreases. Fibers with 0.5 LH/core unfold by forming a two-stack conformation (dominant $i \pm 2$ contacts in Figure 5c) with a limited presence of superbeads, followed by an irregular array with dominant $i \pm 1$ contacts at 10 pN. LH removal thus offers greater conformational flexibility for local adjustments and loosens the chromatin fiber.

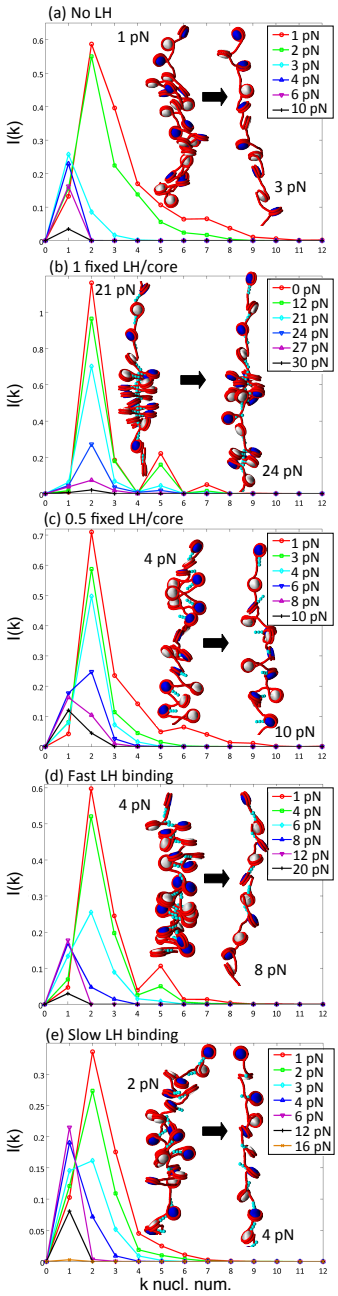

Supporting Figure 5: Unnormalized internucleosome interaction patterns for 24-unit oligonucleosome 209-bp chains at 0.15 M monovalent salt: (a) no LH, (b) 1 LH/core, (c) 0.5 LH/core, (d) fast LH binding, and (e) slow LH binding. The patterns help interpret the transition between structures with diverse dominant internucleosome contacts. Representative simulation snapshots (space filling models) are shown to illustrate structural transitions.

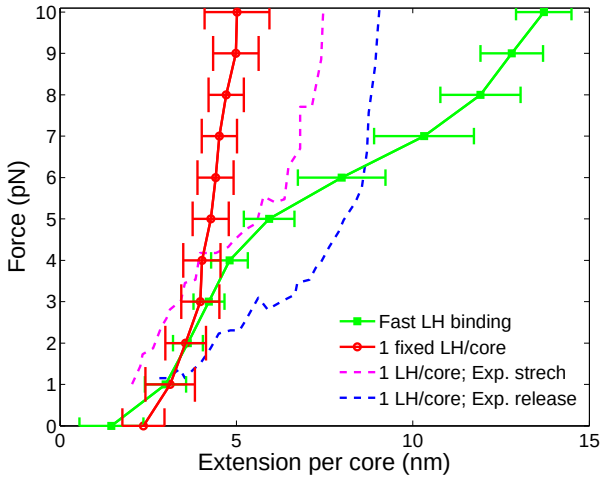

Supporting Figure 6: Simulation and experimental force-extension curves of single chromatin fibers. For comparison purposes the extension is divided by the total number of nucleosomes in each fiber. The solid lines represent simulation results of this work (discussed in detail in the main text) for 24-core 209-bp fibers at 0.15 M monovalent salt with: 1 fixed LH/core (red) and fast LH binding molecules (green). The dashed lines represent experimental stretch (magenta) and release (blue) curves for 280-core 210-bp fibers with LH at 0.04 M monovalent salt taken from (28).